Understanding Na + Diffusion, Physicochemical Behavior, and Electrochemical Performance of a Gel Polymer Electrolyte

Théo Vallier, Rafael Bianchini Nuernberg, Sébastien Issa, Jean-Louis Ferrandis, Lorenzo Stievano, Bruno Ameduri, Vincent Lapinte, Laure Monconduit

Understanding Na^+ diffusion, physico-chemical behavior and electrochemical performance of a Gel Polymer Electrolyte

Théo VALLIER[1,2], Rafaël NUERNBERG[1,2], Sébastien ISSA[3], Jean-Louis FERRANDIS[3], Lorenzo STIEVANO[1,2], Bruno AMEDURI[1], Vincent LAPINTE[1,2], Laure MONCONDUIT[1,2]

[1] ICGM, Univ. Montpellier, CNRS, ENSCM,1919 route de Mende, 34293 Montpellier, France

[2] Réseau sur le Stockage Electrochimique de l'Energie (RS2E), CNRS, 15 rue Baudelocque, 80000 Amiens, France

[3] PELLENC Energy S.A.S, Quartier Notre Dame, Route de Cavaillon, 84120 Pertuis, France

theo.vallier@etu.umontpellier.fr, rafael.nuernberg@umontpellier.fr, s.issa@pellenc-energy.com, jl.ferrandis@pellenc.com, lorenzo.stievano@umontpellier.fr, bruno.ameduri@enscm.fr, vincent.lapinte@umontpellier.fr, laure.monconduit@umontpellier.fr

corresponding author : laure.monconduit@umontpellier.fr

Abstract: Gel Polymer Electrolytes (GPEs) represent a credible alternative to organic liquid electrolytes (LEs) for safer sodium metal batteries. As compromise between solid polymer electrolytes and LEs, GPEs ensure a good ionic conductivity, improve the electrolyte/electrode interface and prevent from solvent leaks. Herein, a GPE based on acrylate-bifunctionalized polyethylene glycol chains mixed with an ether solvent (TEGDME) and a polyethylene glycol diacrylate (*PEG600DA*) in a 50/50%wt ratio was prepared by ultra-violet photopolymerization. Sodium bis(fluorosulfonyl)imide salt (NaFSI) was added at different concentrations to study its interactions with the solvent and/or the cross-linked polymer. Infrared spectroscopy, thermogravimetric analysis, differential scanning calorimetry and swelling ratio

characterizations were combined to determine the physico-chemical properties of the GPE. Complementary characterizations as electrochemical impedance spectroscopy, chrono-potentiometry and cyclic voltammetry allowed correlating the physico-chemical properties of the GPE to its electrochemical performance. Then improvements were obtained by a careful combination of its components. The cross-linking agent allows obtaining a polymer matrix that traps the organic solvent and prevents leakage. Such a solvent inclusion reduces the rigidity of the membrane and lowers its viscosity, offering a room temperature ionic conductivity of 4.8 x 10^{-4} Ω^{-1} cm^{-1}. The control of polymer's tortuosity leads to a stable cycling vs. sodium metal over several hundred hours without increase of the polarization. Finally, the optimization of the salt loading plays a major role in electrostatic cross-linking, leading to an improvement of the mechanical properties of the GPE without reducing its conductivity.

Key words: Gel polymer electrolyte, sodium metal battery, cross-linked polymer, swelling rate, electrochemical impedance spectroscopy, UV curing, concentration dependance

1. Introduction

Today, the growing demand of energy storage is driven by the growing need of portable power tools, as well as by the development of the electric vehicle and stationary storage markets. So far, lithium-ion batteries (LIBs) have been the ideal candidates thanks to their high energy density (100-265 $Wh.kg^{-1}$) and power density, life span and low self-discharge. Unfortunately, the resources of LIB electrode materials, including lithium, cobalt and nickel, are currently depleting. Moreover, almost 30 years after its commercialization, Li-ion technology seems to have reached a limit value in energy density. Replacing lithium with sodium seems to be an excellent alternative to help meeting the demand, since the latter is more abundant and less expensive. However, the energy density of the battery would decrease from 265 to 150 $Wh.kg^{-1}$ in LIBs and SIBs, respectively.[1] A way to increase the energy of Na-based systems is using Na metal as negative electrode in sodium metal batteries (SMB). The high theoretical specific capacity (1166 $mAh.g^{-1}$) of Na, its relatively low redox potential (-2.71 V vs. standard hydrogen electrode), low production cost and abundance make SMB the technology of choice.[2] However, these advantages do not eliminate the safety problems associated with batteries based on metal electrodes (Li, Na, K, etc.). During Na plating, the growth of Na dendrites penetrating through the separator may induce short-circuits, thermal runaway and possibly explosion.[3]

Inhomogeneous sodium stripping during cycling is also known to bring dead sodium with a global loss of active material at the anode. To address these issues commonly encountered with liquid electrolytes (LEs), a possible solution involves replacing them with solid-state electrolytes (SSEs)[3], including solid polymer electrolytes (SPEs)[4]. In fact, SSE are expected to create a physical barrier that limits dendritic growth. Unfortunately, SPEs usually display low ionic conductivity and most of the time need to work at high temperatures. Moreover, SSEs present problems at the electrode/SSE interface originating sluggish Na^+ mobility and polarization. An alternative is represented by polymer gel electrolytes (GPE), a good compromise between SSE and LEs. Consisting of a polymer matrix incorporating the liquid electrolyte, they offer better contact interfaces with the electrodes and higher ionic conductivities, comparable to that of a LE (10^{-3} Ω^{-1} cm^{-1}). One of the characteristics of a GPE for SMBs is its ability to restrict dendrite growth, attributed to the enhanced mechanical properties of the polymer matrix.[1] Based on a study by Monroe and Newman[5] on lithium dendrites, it was possible to approximate that a protective layer having a shear modulus of 5.2 GPa is sufficient to suppress sodium dendritic growth.[6] The polymer matrix will provide mechanical resistance to dendritic growth but also propose a tortuosity due to the high crosslinking density. It will not stop but at least slow down the dendrites by lengthening their travels. Also Khurana *et al.* proved that high-modulus polymer electrolyte is not a requirement for the control of dendrite proliferation.[7] Electrolytes with higher ionic conductivity and reduced anion mobility will delay dendrite nucleation. Battery safety is also enhanced, as trapping the salt and the organic solvent in the polymer prevents solvent leakage and electrochemical instability.[8] These improvements, however, should be achieved while maintaining reasonable ion transport properties (ionic conductivity, transport number and stable plating-stripping over time).

Several recent studies promote the use of GPEs to tackle the challenges faced by SMBs. Among them, Zhang *et al.* propose a poly(butyl acrylate)-based GPE showing a good ionic conductivity (1.6 x 10^{-3} Ω^{-1} cm^{-1} at RT) connected to cation solvation by the polymer as well as the ability of suppressing the formation of sodium dendrites.[8] Murugan *et al.*, on the other hand, suggest the use of a pentaerythritol triacrylate-based GPE in a sulfur cathode to reduce polysulfide shuttle.[9]

This article focuses on the development of a GPE photopolymerized by UV irradiation and provides a comprehensive exploration of its physico-chemical properties and the correlated electrochemical performance in SMBs. Such a GPE is synthesized by cross-linking an T-

functionalized polyethylene glycol (PEG) exhibiting good ionic conductivity (4.8 x 10^{-4} Ω^{-1} cm^{-1}), an electrochemical stability window exceeding 4.1 V and allowing stable plating-stripping in SMBs over more than 200 cycles at 0.01 $mA.cm^{-2}$. In specific, attention is devoted in understanding the interactions among the different GPE components (cross-linked polymer, solvent and sodium salt). This is achieved through a combination of complementary characterization techniques including Thermogravimetric analysis (TGA), Differential scanning calorimetry (DSC), FT-IR spectroscopy and measurement of the swelling rate (SR). Ultimately, the physico-chemical features of GPE membranes are correlate with their electrical properties and electrochemical performances in SMBs and the interplay between them are discussed.

2. Experimental section

2.1 GPE Preparation

The GPE studied in this work was synthesized by UV photopolymerization of a solution containing a di- or triacrylate-functionalized PEG monomer[10], polyethylene glycol diacrylate (PEG600DA) *(Sartomer®)*, a liquid electrolyte composed of an ether solvent, tetraethylene glycol dimethylether (TEGDME) *(Sigma-Aldrich®, >99%)* and a sodium salt, Sodium Bis(fluorosulfonyl)imide (NaFSI) *(Solvionic®, 99.9%),* in different molar concentrations using 2,2-dimethoxy-2-phenylacetophenone (DMPA) *(Sigma-Aldrich®, 99%)* as a photo-initiator.[11] The photo-activation was carried out using a K-ILU 2 UV lamp (KLOÉ) at 365 nm, a UV-LED curing adhesive system with a collimated beam in continuous mode for 3or 5 seconds according to the polymerized samples (**Figure 1**).

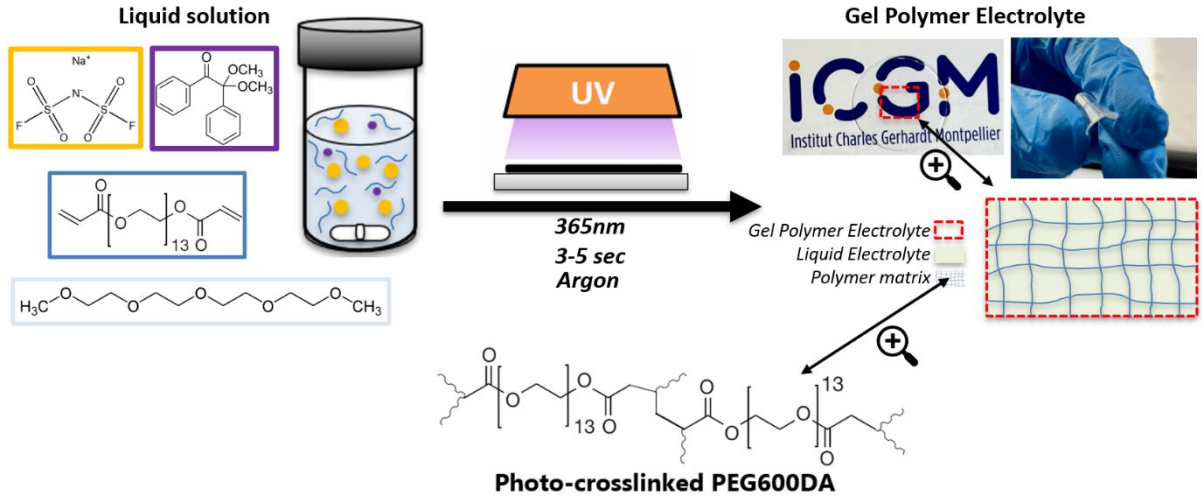

Figure 1. Schematic illustration of the preparation of the gel polymer electrolyte by fast UV-curing of PEG diacrylate based polymer matrix containing TEGDME solvent and NaFSI salt.

2.2 Physico-chemical characterization

Infrared spectra were recorded with a Nicolet™ iS50 FT-IR Spectrometer model in Attenuated Total Reflection (ATR) mode. The conversion of the reactive functions during UV photopolymerization can be followed by the vanishing of the C=C band of the monomer acrylate function (cf. Supporting Information, **Equation S1**).

The swelling rate (SR) of the polymer was measured by immersing the dry cross-linked polymer matrix, obtained by evaporating the solvent from the cross-linked polymer gel in a glass oven under vacuum at 120 °C, into the solvent used in the final GPE for 12 hours (or until the total mass does not vary anymore). SR was assessed from the mass of dry (W_d) and swollen polymer (W_s) according to **equation 1**. SR allows estimating the capacity of the polymer matrix to accept the organic solvent.

$$\text{SR}\ (\%) = \frac{(Ws - Wd)}{Wd} * 100 \quad \textbf{(1)}$$

Flory and Rehner's mathematical theory can be used to relate the swelling of polymer networks with the cross-linking density (also **Equation S2**, Supporting Information). This theory allows tracing the average length between two cross-linked knots, and systematically shows that the SR decreases with increasing cross-linking density.[12]

TGA and DSC analyses were carried out on a TGA Q50 (Thermo Scientific) and on a DSC 3500 Sirius (Netzsch) instrument, respectively. TGA analyses were performed under nitrogen flow at 40 mL.min^{-1} with a temperature ramp from room temperature to 580 °C at a rate of 20 °C.min^{-1}. For the DSC analyses, approximately 10 mg of sample was placed in a perforated aluminium mould. Thermal properties were recorded between -100 and 100 °C at a rate of 10 °C.min^{-1} for samples with TEGDME solvent and from -100 to 200 °C at 10 °C.min^{-1} for cross-linking PEG600DA samples. The reported glass transition temperature (T_g) and melting temperature (T_m) values are those obtained during the second heating ramp.

2.3 Electrochemical characterization

The electrochemical measurements were made in half cells, easier to use, however the use of a stable reference would be necessary to avoid measurement drift, due to the instability of the sodium metal electrode used as RE.[13]

The electrochemical stability of the electrolytes was studied by cyclic voltammetry (CV) over the potential range 0 – 5 V *vs.* Na^+/Na with a sweep rate of 0.1 $mV.s^{-1}$ at room temperature using a BioLogic VSP potentiostat on (Na | GPE | SS) 2032-type non-symmetric coin cells with a SS (Stainless Steel) working electrode and a Na metal as both reference and counter electrode.

Polarisation tests were carried out in symmetric Na | GPE | Na cell configuration (2032-type coin cells) by applying a constant current density of ±0.01 $mAh.cm^{-1}$.

The ionic conductivity of different electrolytes was determined by electrochemical impedance spectroscopy (EIS) in the frequency range from 1 MHz to 10 Hz with an amplitude of 10 mV using a BioLogic VSP potentiostat. The measurements were carried out in symmetric Swagelock-type cells, with a GPE disk (9 mm diameter, 400 µm thickness) sandwiched between two SS electrodes. This protocol was also used at variable temperatures between 30 and 90 °C with the cell placed in a thermostatically controlled oven.

Chronoamperometry (CA) measurements coupled with potentiostatic EIS (PEIS) were used to determine the Na^+ transport number in different electrolytes by applying a polarization of 20 mV for 10 h after leaving the cell resting for 20 h at open circuit voltage (OCV). PEIS measurements were carried out two times: firstly after OCV and secondly after polarization steps, once the potential stabilized with an amplitude of 20 mV using a BioLogic VSP potentiostat. The measurements were performed using symmetric 2032-type coin cells using a polymer electrolyte disk (diameter 16 mm and thickness around 400 µm) sandwiched between two sodium metal electrodes with a diameter of 14 mm. All cells were prepared in a glove box under argon atmosphere at room temperature.

3. Results and discussion

3.1. Physico-chemical properties of GPE synthesized by UV photopolymerization

Transparent GPE samples were prepared by photopolymerization of PEG di-or triacrylate in a stainless-steel mold and under a controlled atmosphere[14] (Supporting information, **Figure S1** for more details). In order to optimize the synthesis conditions, several parameters such as the irradiation time, the temperature, the power of the UV lamp, the distance between the lamp and the sample, the amount of monomer as well as the thickness of the sample were investigated.[15–17] The degree of conversion (DC) of the C=C bonds was optimized with the aim of preventing membrane degradation (cracks or yellowing the membrane) by prolonged UV irradiation. SPEs contain twice as initial monomers and photoinitiator amount than GPE, resulting radical species

propagate more rapidly. In all cases, transparent cross-linked membranes incorporating the liquid electrolyte were obtained. The physicochemical properties of the synthesized GPEs, evaluated as a function of the NaFSI concentration, are reported in **Table 1**.

Table 1. Physico-chemical and thermal properties for cross-linked PEG600DA-based (P6) Gel Polymer (GP, without salt) containing TEGDME in the ratio 50-50 %wt, GPEs containing TEGDME in the ratio 50-50 %wt with different ratio of NaFSI and SPE with 0.1M NaFSI (without solvent).

Sample	NaFSI [mol.L^{-1}]	UV irradiation (s)	$DC_{C=C}$ (%)	SR (%)	Degradation starting temperature (°C)[a)]	Polymer degradation range (°C)[a)]	T_g (°C)[b)]	T_m (°C)[b)]
GP_P6	0	5	30	110	95	325-425	-53	82
GPE_P6[0.1]	0.1		40	46	95	360-440	-64	82
GPE_P6[0.2]	0.2		50	42	95	360-440	-65	82
GPE_P6[0.5]	0.5		50	42	95	300-425	-66	82
GPE_P6[1]	1.0		53	32	95	300-425	-67	82
SPE_P6[0.1]	0.1	3	67	46	/	360-440	-38	78

a) from TGA analysis (N_2, 20°C.min^{-1}); b) from DSC analysis (N_2, 10°C.min^{-1})

The efficiency of the cross-linking of the membranes was checked by FT-IR spectroscopy and swelling rate tests. This latter method allows controlling the incorporation of liquid electrolyte in the polymer matrix, also assessed by TGA. The FT-IR spectra of the films prepared from different monomer/solvent ratios, variable salt concentrations (see Table 1), as well as before and after UV photopolymerization are displayed in **Figure 2.** The progression of UV photopolymerization can be followed by monitoring the disappearance of the C=C band associated with the acrylate function of the monomer[10], observed at 1630 cm^{-1} (**Figure 2a**). **Figure 2b** provides complementary information on the conversion of the acrylate with the decrease of the characteristic peak of C=C-H bond at 988 cm^{-1}. In the specific case of photopolymerization of liquid monomers the conversion can be quantified using **Equation S1** (cf. Supporting Information).[18] The calculated DCs are gathered in **Table 1** and show that the lower the solvent amount in the sample, the better the degree of conversion.

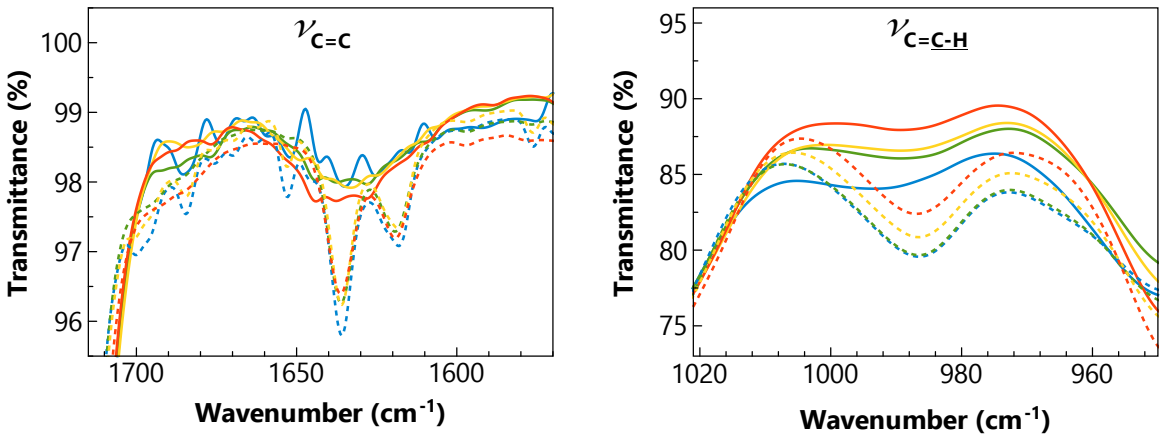

Figure 2. Characteristics peaks of the acrylate group in the FT-IR spectra of the GPEs before (dotted lines) and after (solid lines) UV curing at different salt concentrations (blue=0.1 M, green=0.2M, yellow=0.5M and red=1M).

The SR of dry cross-linked polymer matrices prepared from two different monomers with varying monomer/solvent ratios (**Figure 3**) was used to assess their ability to confine the liquid electrolyte within them.[19] A strong decrease of the SR with increasing relative amount of monomer is observed for PEG600DA (1D), whereas the value of the SR is very low and almost independent of the monomer/solvent ratio for Ethoxylated (15) Trimethylolpropane Triacrylate TMP15EOTA (3D), confirming the influence of the number of acrylate-PEG functionalization on the SR. The linear agent can host more than two times its weight in solvent (SR>100%), whereas the 3D agent accepts only one tenth of its weight in solvent (SR<10%). The cross-linked polymer matrix obtained using a 50/50 wt.% mixture of the two monomers shows a behavior close to that of the PEG600DA-based one. The inclusion of PEG600DA in the polymer network enables the formation of cross-linking knots in two directions within the same plane in addition to the phenomenon of polymer chain entanglement. This phenomenon is limited in our case due to the short chain length between two cross-linking nodes. In contrast, TMP15EOTA provides three directions, forming naturally cross-linked knots that promote a higher cross-linking density. Decker explains that cross-linked acrylate-based polymers composed of trifunctional acrylates exhibit resistance to breakage and low elongation, reaching a hardness close to that of glass.[15] The chain length between theoretical cross-linking knots is crucial for cross-linking, with triacrylate featuring a length half that of diacrylate (5 and 13 repeat units, respectively), resulting in closer knots and higher cross-linking density. These results indicate PEG600DA as the most adapted monomer for obtaining a good GPE, given its better liquid electrolyte confinement properties. To maintain a certain rigidity of the matrix and

ensure the effective inclusion of the solvent within it, a 50-50 monomer/solvent ratio was selected.

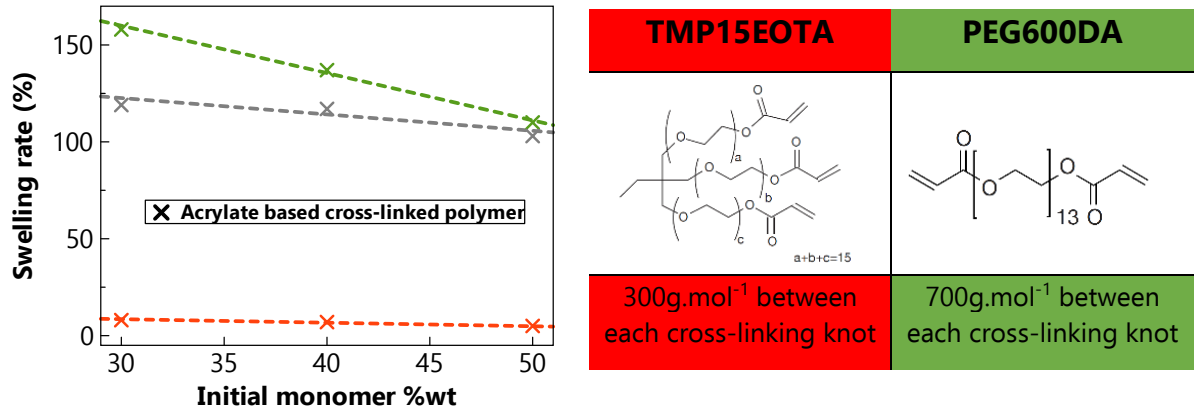

Figure 3. SR (%) as a function of the monomer %wt for the diacrylate ZPEG600DA (green) and the triacrylate TMP15EOTA (red) monomers. The SR of a 50-50 wt.% diacrylate-triacrylate mixture (grey) is also shown for comparison.

The influence of the salt concentration on the SR was also studied by soaking the SPE composed of polymer matrix and sodium salt in TEGDME until no variation of the swollen mass is observed. **Figure 4** shows the variation of SR as a function of sodium salt concentration and amount of monomer in the SPE. The SR decreases with increasing sodium salt concentration showing the direct influence of the salt on the network rigidity. This trend is counter-intuitive at a first glance compared with the results previously shown in **Figure 3.** Nevertheless, Na^+ ions can induce electrostatic cross-linking between polymer chains by interacting with the oxygens in PEG chains, thereby inducing the formation of an additional network.[20] **Figure S2** shows characteristic peak associated to the vibration of the C-O-C polymer bound shifted to lower frequencies in the presence of salt. This shift is attributed to the EO-Na^+ interactions of electrostatic cross-linking, resulting in a decrease in the vibrational frequency of C-O-C stretching.[20] This shift is intensified with increasing salt concentration confirming interactions between sodium cation and oxygens of the polymer matrix. Electrostatic cross-linking is

highlighted, with a loss of mobility due to the creation of a new network. Resulting the -EO units moving closer together around the sodium cation. **Figure 4** highlights this phenomenon. Even with a reduced cross-linking agent amount, the cross-linking density increases concomitantly, indicating that the cross-link agent is not the only component that control cross-linking density of the resulting film.

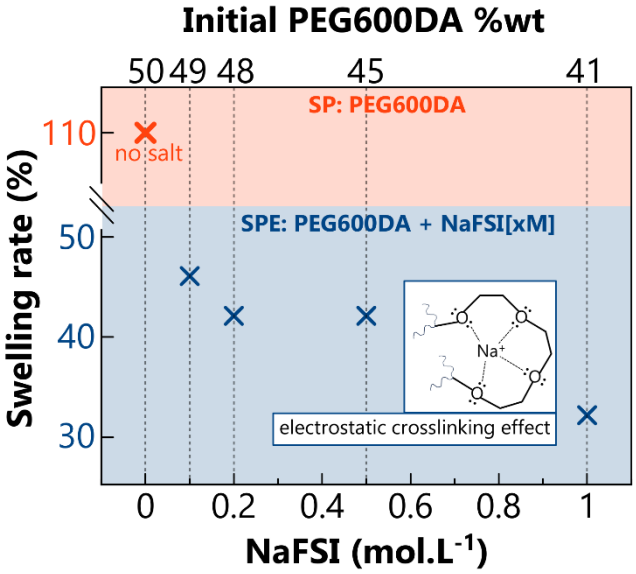

Figure 4. Salt concentration dependence of SR values for a diacrylate based SPE.

Infrared spectroscopy was used to follow the influence of sodium salt concentration and monomer/solvent ratio on the cross-linking density of the GPE system. As shown in **Figure 5**, the change in concentration of the NaFSI salt in a system with a fixed monomer/solvent ratio of 50-50 wt.% produces a visible change in intensity of several spectral features. The intensity of the characteristic peaks of the NaFSI salt at 1370 and 1182 cm^{-1} (corresponding to S=O and S=O stretching, respectively) increases with its molar concentration, and simultaneously those of solvent and monomer at 1725 cm^{-1} (C=O) and 2870 cm^{-1} (C-H) (Supporting information, **Figure S3**) decrease. Interestingly, a new band appears at 826 cm^{-1} which does not correspond to any characteristic band of solvent or monomer, and grows in intensity with the salt concentration. This new band can be attributed to the FSI anion of the salt, shifted from 846 to 826 cm^{-1}, confirming its possible strong interaction with the GPE wich can reduce the fluorinated anion mobility.[21] It should be noted that here we compare IR spectra of a salt in powder form and a salt dissolved in a solvent trapped in a polymer matrix. This may affect his conformation.

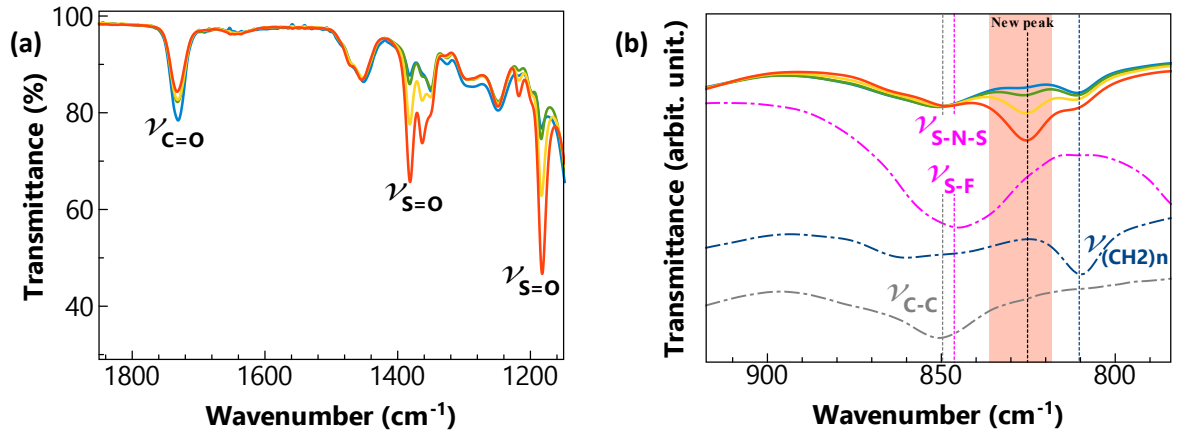

Figure 5. FT-IR spectra of the GPEs after UV curing at different salt concentrations (blue=0.1 M, green=0.2M, yellow=0.5M and red=1M) in (a) 1150-1800-cm^{-1} and (b) in 780-920 cm^{-1} regions. The region of the FSI anion vibrations is highlighted (NaFSI in pink, PEG600DA in dark blue and TEGDME in gray).

The addition of a salt to a polymer-solvent system impacts both cross-linking density and interactions among compounds, with observable effects on the salt-polymer and salt-solvent interactions. These interactions could also influence the thermal stability of various electrolyte systems. In **Figures 6** and **7**, TGA thermograms (and corresponding derivative) of the GPE is compared to that of its components: solvent, salt, and polymer. Despite a rigorous approach to drying salt, careful storage of the components and working in the most controlled atmosphere possible, we have a small amount of water remaining in the samples. In **Figures 6** and **7**, TGA thermograms (and corresponding derivative) show a persistent water content of less than 1%. likely due to the transfer from the glove box to the TGA, resulting in this low water absorption. However, in the battery assembly process, the polymer electrolyte does never leave the glovebox. The first mass loss from 95 to 205 °C is then related to the TEGDME solvent, the second one from 210 to 350 °C is related to the FSI anion and the third one from 325 to 450 °C is due to the cross-linked PEG polymer. The small residual mass above 500 °C represents amorphous carbon remaining after incomplete GPE decomposition. A few substantial differences are detected between the thermograms of GP and LE, showing that the presence of the salt influences solvent degradation. The shift of the derivative peak corresponding to the loss of solvent from 155 to 180 °C after addition of the salt is the consequence of the solvation of the latter by TEGDME, likely via hydrogen bonding and/or van der Waals interactions. At higher temperatures, the derivative peak of the polymer moves from 400 to 420 °C with the addition of the salt, confirming the occurring of electrostatic cross-linking (*vide supra*) via the

chelation of Na^+ with the ether units of the polymer causing the rigidification of the matrix and the improvement of its thermal stability.

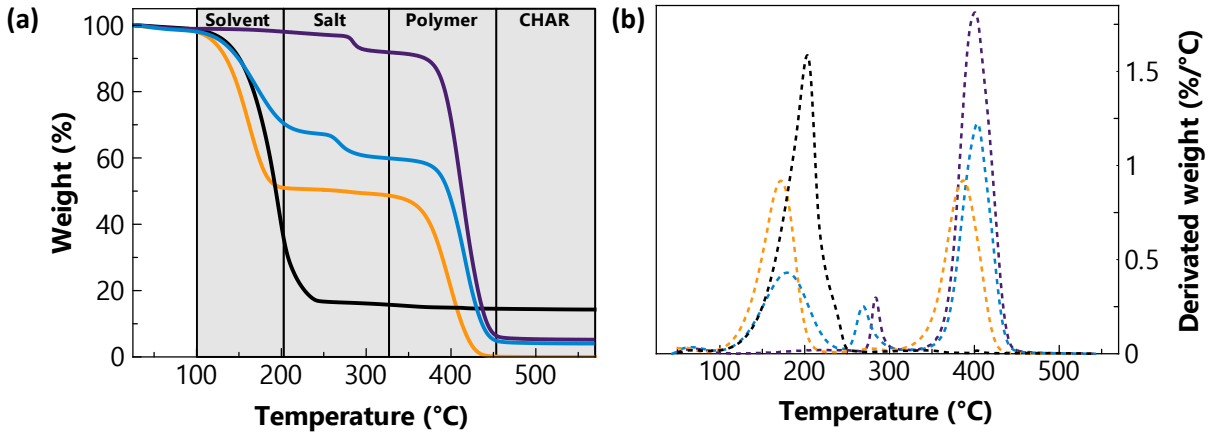

Figure 6. (a) TGA curve and (b) corresponding derivatives for cross-linked PEG600DA, TEGDME and NaFSI in different electrolytes: GP (orange), LE 0.1M (black), SPE 0.1M (purple) and GPE 0.1M (blue).

The TGA signals of GPEs prepared with different salt concentrations, providing information about the influence of the amount of salt on their thermal stability, are shown in **Figure 7**. For the two least concentrated systems (0.1 and 0.2 M), mass losses corresponding to solvent, salt and polymer degradation occurs at distinct temperatures. For the more concentrated 0.5 M sample, the mass loss of the polymer around 400 °C represents only 22 wt.%, while a mass loss of 45 wt.% is theoretically expected. This discrepancy can be explained by the partial degradation of the polymer matrix already at lower temperatures, possibly at the same time of the degradation of the salt anion, as confirmed by the continuous mass loss observed from 260 to 425 °C for the 1 M sample. The strong interaction with the salt stabilizing the polymer matrix, as detected by SR measurements (cf. **Figure 4**) rather seems to be detrimental to the thermal stability when the salt concentration exceeds 0.5 M. This behavior can be explained by a nucleophilic attack of FSI anion on the cross-linked network that bears several electrophilic sites wich might favor the degradation of the GPE. Actually, Cheng et al. reported that high LiFSI concentrations in 1,3-dioxolane (DOL) induced an in situ ring-opening polymerization (ROP). Poly-DOL is produced without any external stimuli conditions leading to an increase of the thermal stability.[22] ROP is due to the nucleophilic attack of FSI anion onto DOL electrophile site. In our case, the same mechanism seems to occur causing a destabilization of the cross-linked network. This would lead to its ring opening, resulting in the formation of low-molar mass-polymers not attached to the cross-linked network. To address this ambiguous impact of

salt on the physicochemical properties of GPE, further physicochemical characterizations were carried out.

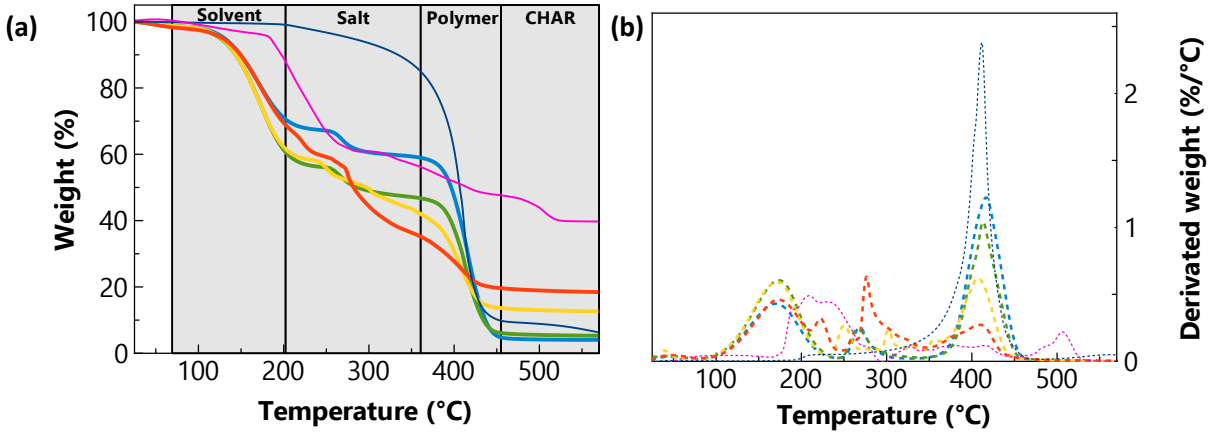

Figure 7. TGA thermograms (a) and corresponding derivative (b) of GPEs containing different salt concentrations (blue=0.1 M, green=0.2 M, yellow=0.5 M and red=1 M) compared to cross-linked PEG600DA (dark blue) and NaFSI (pink).

In addition to TGA, DSC was used to deepen the understanding of the physico-chemical properties of the GPEs. The DSC curves centered around the glass transition temperature (T_g) and the melting temperature (T_m) of the GPEs containing different amounts of NaFSI are shown in **Figure S54** together with those of other reference materials: GP, SPE and Solid Polymer (SP). The evolution of T_g allows following the plasticizer effect of the differents compounds in the GPE.

First of all, the peak at -30 °C is characteristic of the melting temperature of TEGDME (Supporting information, **Figure S5**). TEGDME plays the role of plasticizer, reducing the T_g from -37 to -53 °C on going from the SP to the GP. TEGDME is known to play several roles in GPEs (solvent, oligomer and plasticizer) and it is frequently used in PEG-based PEs. Many studies describe its ability to lower the crystallinity of semi-crystalline PEG.[23,24]

A further decrease of the T_g from -53 to -66 °C is observed upon addition of the salt, in line with the role of plasticizer also played by the FSI anion. Indeed, previous studies on TFSI, similar to FSI, show the existence of two stable geometrical conformations obtained by rotation of the ion around the S-N bonds, separated by a small activation barrier. The flexibility of FSI thus lowers the rigidity of the system, leading to a decrease of the glass transition temperature.[25]

If the increase of the salt concentration is supposed to weaken the thermal stability of the GPE, here it does induce a significant modification of the T_g, which is -66 °C for 0.1, 0.5 and 1 M and -72 °C for 0.2 M NaFSI concentrations. Indeed, with the increase of the amount of salt, the amount of polymer decreases and sodium chelation also plays a role which should lead to an increase of T_g. The opposite effect of these two phenomena may therefore explain the observed constant value of the T_g.

In the 40-110°C range, a rather weak endothermic transition is observed around 70 °C (Supporting information, **Figure S4**). According to the literature, this transition should correspond to the T_m of semi- crystalline PEGs.[26] Nevertheless, the observed variation of the DSC base line is extremely small compared with the melting peak found for a PEG:NaTFSI polymer electrolyte by Moreno *et al.* in their study[26]. The outcome of this comparison implies a low level of crystallinity in SP, SPE, GP and GPEs membranes synthesized in this study. The cross-linking of the polymer matrix by means of the cross-linked agent is likely to be the main reason for the low crystallinity achieved in the obtained membranes. Working on high molecular weight linear PEG polymers cross-linked with trifunctional azide groups, Golitsyn *et al.* showed that the crystallinity rate increases with the molar mass of a linear PEG.[27] In particular, they showed that the crystalline zones are located around the PEG chains, whereas the amorphous zones are rather related to the cross-linking knots.[13] The low intensity T_m observed here might be the result of a similar effect, with the amorphous portion of the material predominant around the cross-linking knots, and the low crystallinity ensured by the remaining linear PEGs chains that are long and near enough to crystallize. It is also worth to note that, the addition of NaFSI shifts the T_m to higher temperatures in all membranes, possibly because of the previously detected electrostatic cross-linking phenomena caused by Na^+ affinity with the oxygens of PEG chains.

3.2. Electrical and Electrochemical properties of GPE

The electrical properties of the GPEs with distinct NaTSI concentrations were followed by EIS and compared to those of reference systems, including SPE and LE at low salt concentration (0.1 M). The Nyquist plots for LE, SPE and GPE samples measured at 303 K are shown in **Figure 8**. At a first glance, the impedance response of SPE, GEL and LE is characteristic of ion-conducting electrolytes, with a straight and steep increase of the imaginary part of impedance (spike) at low frequency. This low-frequency response is commonly denoted as a

polarization effect and is due to the blockage of mobile ions at the interface between electrolyte and metallic electrodes.[28] Herein, the complex impedance data (Z*) have already been normalized regarding the shape factor of each sample (L/A, where L and A represent the thickness of the electrolyte and electrodes area, respectively) to get the specific impedance Z*S (Z*S = Z*/(L/A)), so that the impedance response of the samples can be directly compared. Hence, the resistivity of the samples can be roughly read by extrapolating the low-frequency spike towards the X-axis as the intercept the real part of the specific impedance (ZS'). Roughly, the SPE (**Figure 8a**) is almost three orders of magnitude more resistive than the LE (**Figure 8a**) while the GPE (**Figure 8b**) is only one order of magnitude more resistive than the LE. Regarding the influence of the salt concentration on GPE membranes, the resistivity tends to decrease systematically with the increase of NaFSI concentration, down to the approximately the same resistivity of the LE 0.1M in the case of the GPE 1M membrane.

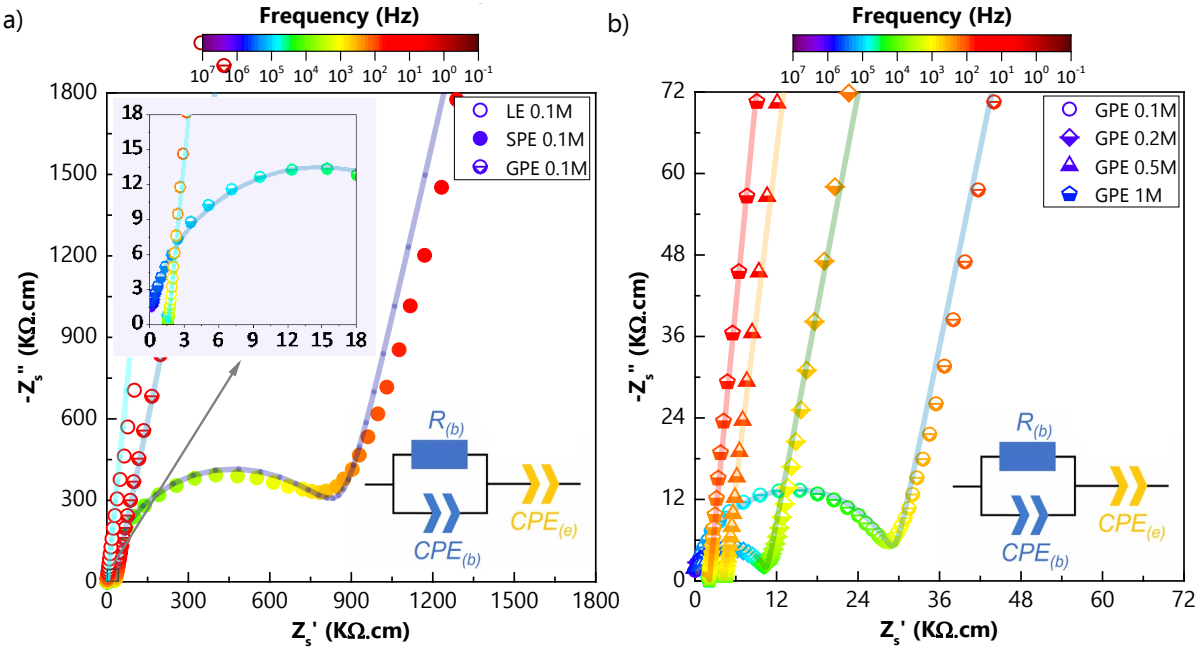

Figure 8. Nyquist plots of LE, SPE and GPE (a) with distinct salt concentrations (b) recorded at 303 K. The complex impedance data were previously normalized regarding the shape factor of each sample in order to allow the direct comparison between samples. Insets show the associated equivalent circuit used to fit the impedance data. Letter R and acronym CPE represent resistive and constant phase circuit elements, respectively, while subscripts b and e denote bulk and electrodes responses, respectively.

The impedance data were fitted applying an appropriate equivalent circuit (**Figure 8**) to determine precisely the resistivity (ρ) and consequently the conductivity (σ = 1/ρ) of the

materials. This procedure was conducted for measurements carried out at distinct temperatures (**Figure S6**). **Figure 9** depicts the dependence of the ionic conductivity on the temperature for GPE membranes with distinct NaFSI concentrations as well as LE and SPE. Remarkably, the temperature dependence of the ionic conductivity for all samples follows a super-Arrhenius behavior characteristic of a liquid-like diffusion mechanism, in which the viscosity controls the diffusion process (**Figure 9**). This behavior is typical of liquids or polymer electrolytes in temperatures ranges above T_g. The increase of temperature enhances the movement of polymeric chains and solvent molecules, decreasing the viscosity of the system and increasing the ionic conductivity. The dependence of the ionic conductivity on the temperature can be properly fitted employing a Vogel−Fulcher−Tammann (VFT) relation (**Equation 2**)[29]:

$$\sigma = \sigma_0 \, e^{\left(\frac{-B}{k_B(T-T_0)}\right)} \quad \textbf{(2)}$$

where k_B is the Boltzmann constant, T the absolute temperature and σ_0, T_0 and B are fitting parameters, respectively denoted as the pre-exponential factor, the ideal glass transition temperature and the activation energy associated to the transport mechanism.

As expected, the liquid electrolyte shows better ionic conductivity than GPE and SPE membranes due to its lower viscosity. Besides, the ionic conductivity can be improved by increasing the molar concentration of NaFSI, at least up to 1 M. Since the ionic conductivity is directly related to the number of free charged species (n_i) in the system (**Equation S4**), the increase in salt concentration is expected to enhance the conductivity. However, increasing salt concentration could also increase the viscosity, therefore leading to a decrease of the ionic mobility (μ_i) with a detrimental impact on ionic conductivity (**Equation S4**). This is probably the reason why the increase in NaFSI concentration from 0.1 to 0.2 M causes a greater improvement in conductivity than increasing the concentration from 0.5 to 1 M. Boschin A. and Johansson P. demonstrated in a study that increasing the NaFSI salt concentration in a PEO-based polymer electrolyte had an influence on the amount of Na^+-FSI^- contact ion pairs and therefore intrinsically of free anions. A certain amount of salt would result in 22% of the salt being in the form of aggregates inside SPE.[30] This may also explain why the increase in ionic conductivity is lower between 0.5M and 1M than between 0.1M and 0.2M. Moreover, as discussed above, the NaFSI concentration can also increase electrostatic cross-linking (**Figure 4**), and therefore the cross-linking density of the system, reducing the space between PEG chains. In a SPE, this leads to an increase in T_g which is a consequence of a decreasing in segmental mobility.[20] In a GPE, this phenomenon is attenuated by the presence of solvent which

acts as a plasticizer (Supporting information, **Figure S4**) reducing the viscosity of the system and therefore increasing ion mobility. Therefore, the solvent-polymer affinity in this system seems to increase the degree of freedom inside the polymer matrix favoring ionic transport. It is also important to mention that no transition in the ionic-conductivity behavior is observed around T_m (**Figure 9**), corroborating the hypothesis that the crystalline fraction in SPE and GPE electrolytes should be marginal. Conversely, in PEO-based SPE employing NaFSI as salt, Kumar et al. observed an important increment in conductivity under heating while approaching T_m, featuring two different regimes with distinct activation energies.[31] As summarized in **Table 2**, the GPE membrane with 0.1 M NaFSI concentration presents an intermediate room temperature ionic conductivity between those of SPE and LE membranes. Finally, the high concentrated gel polymer electrolyte (GPE with 1 M NaFSI) exhibits comparable room temperature ionic conductivity that of LE with 0.1 M NaFSI (**Table 2**).

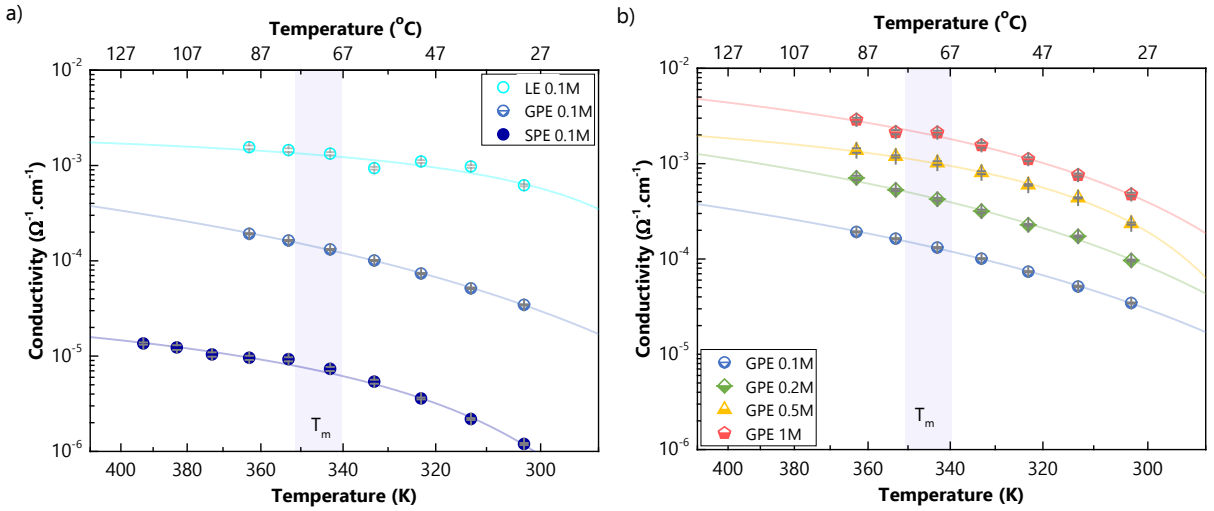

Figure 9. Dependence of ionic conductivity on the temperature for LE 0.1 M, SPE 0.1 M (a) and GPE membranes with 0.1, 0.2, 0.5 and 1 M NaFSI concentrations (b). The ionic conductivity data shown here have been fitting applying the so-called VFT equation.

Table 2. Electrochemical properties for TEGDME based LE with 0.1M NaFSI, cross-linked PEG600DA-based (P6) GPEs containing TEGDME in the ratio 50-50 %wt with different ratio of NaFSI and SPE with 0.1M NaFSI (without solvent).

Sample	NaFSI [mol.L^{-1}]	UV irradiation (s)	σ (Ω^{-1} cm^{-1}) at 25°C	t+	Overpotential PS (V) at 0.01mA.cm^{-2} after 300 hours	Stability range(V)
LE	0.1	-	6.2 x 10^{-4}	-	-	3.6
GPE_P6[0.1]	0.1	5	3.5 x 10^{-5}	-	1.5	4.1
GPE_P6[0.2]	0.2		1.0 x 10^{-4}	-	0.25	4.1

GPE_P6[0.5]	0.5		1.8×10^{-4}	0.4	0.15	4.1
GPE_P6[1]	1.0		4.8×10^{-4}	0.5	0.075	4.1
SPE_P6[0.1]	0.1	3	1.2×10^{-6}	-	-	-

The transport number (t^+) is another important parameter that has to be taken into account to determine the effective Na^+ conductivity. Several measurement methods are proposed in literature but their applicability needs to be verified according to the system studied.[32,33] As shown in **Figure S8**, for lower NaFSI concentrations, the interface resistance does not stabilize even after 100 h, while it does after 20 h for higher concentrations. This continuous increase in of the interphase resistance is likely due to the formation of non-passivating solid electrolyte interphase (SEI), normally constituted of organic and inorganic byproducts originating from the salt and solvent degradation.[34] Consequently, for membranes with low NaFSI concentrations, such calculation methods are not suitable because reliable resistance values at the interfaces are necessary to calculate t^+. Thus, the Na^+ transport number are obtained only for GPE membranes 0.5 and 1 M employing the Bruce and Vincent method[32], which gives values (**Table 2**) in reasonable accordance with those fond for PEG:NaTFSI polymer electrolytes[26].

Figure 10 shows the galvanostatic polarization test of a symmetric Na|GPE|Na cell. After 20 h at OCV conditions, positive and negative current were alternatively applied over 350 hours. Every few cycles, EIS was applied to follow the evolution of the electrode-electrolyte interface, and indirectly get information about electrolyte degradation. The potential of the cell with the 0.1 M NaFSI GPE at 0.01 mA/cm^2 gradually increases, to reach 1.5 V after 300h, while GPEs with higher salt concentrations show a sensibly lower polarization, limited to 0.25 V after 300 h (**Table 2**). The best result is obtained at 1 M concentration, with a stable polarization below 0.075 V after more than 300 h of cycling (**Table 2**). The shape of crenellations describes a homogeneous removal and deposition of sodium, also that dendrite growth has been blocked.[3]

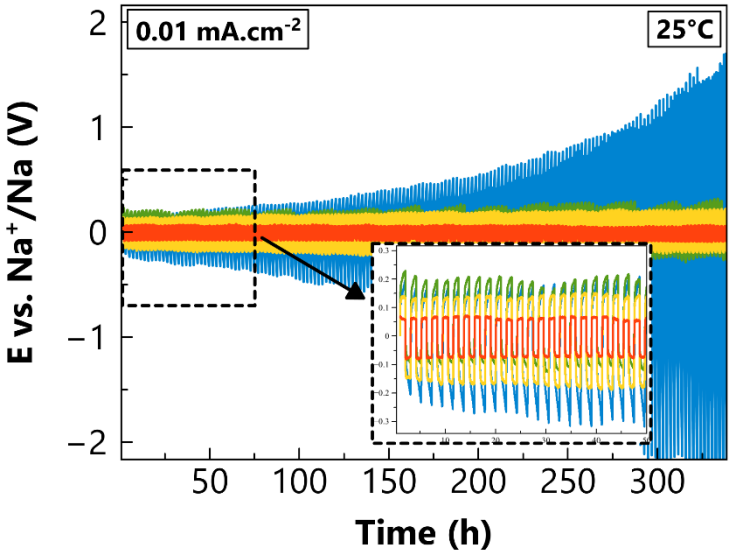

Figure 10. Na plating/stripping in the Na||Na symmetric cells with GPEs at different salt concentrations (blue=0.1 M, green=0.2 M, yellow=0.5 M and red=1 M) for a current density of 0.01 mA.cm^{-2}.

To investigate the electrochemical stability window of the GPEs, linear sweep voltammetry (LSV) measurement was carried out from 3 to 4.5 V vs Na^+/Na at a scan rate of 0.1 mV s^{-1} at 25°C (**Figure 11**). The anodic decomposition of the GPE occurs around 4.1 V, 0,6 V higher than for LE, and is practically independent of the NaFSI concentration (**Table 2**). The addition of the polymer is beneficial for the protection of the sodium anode, limiting the salt decomposition on the electrode.[35] These GPEs can therefore be used as electrolytes for SMBs operating at 4.1 V.

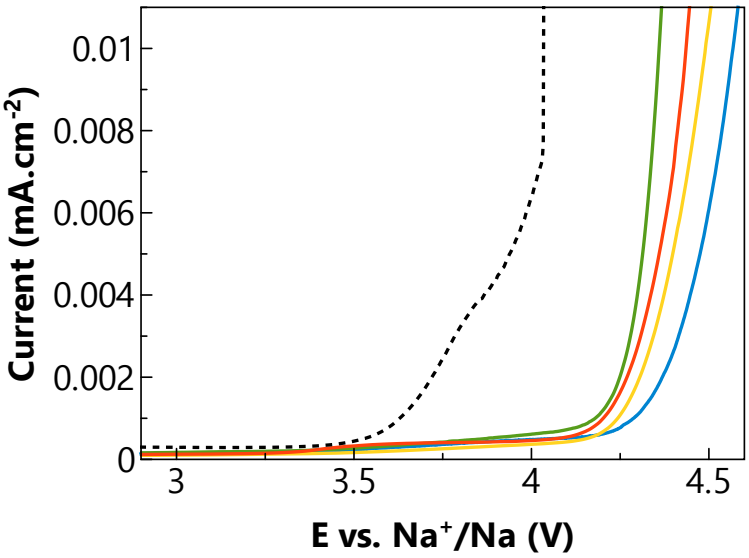

Figure 11. LSV in the Na|electrolyte|SS cells with LE [0.5M NaFSI] (dotted line) and GPEs (solid lines) electrolyte at different NaFSI salt concentrations (blue=0.1 M, green=0.2 M, yellow=0.5 M and red=1 M) at a scan rate of 0.1 $mV.s^{-1}$ at 25 °C.

Conclusion

A new GPE for SMBs containing NaFSI and TEGDME incorporated within a cross-linked polymer matrix, characterized by a high ionic conductivity of 4.8 x 10^{-4} Ω^{-1} cm^{-1} at 25 °C, was prepared by UV photopolymerization of an acrylate-functionalized PEG monomer. Thermal characterization by TGA and DSC showed that the presence of the salt delays termic degradation of both the polymer, thanks to electrostatic cross-linking, and the solvent, thanks to solvation. The increase of salt concentration, however, produces an embrittlement of the polymer structure. SR measurements revealed the influence of the monomer/solvent ratio on the cross-linking density in the membrane, with lower degree of freedom at high monomer/solvent ratios, which also decreases the ability of the polymer matrix to incorporate the liquid electrolyte in the final GPE. The salt influence on the SR also confirmed the presence of electrostatic cross-linking between the Na^+ cations and the cross-linked polymer matrix. The increase in salt concentration stabilizes the sodium electrode-GPE interface at 25 °C. Such GPE is characterized by a higher stability than that of a similar LE (GPE ~ 4.1 V vs. LE ~ 3.5 V), as detected by LSV. The observed interactions between the three components of the GPE, *i.e.*, the polymer, salt and solvent, underlined the importance of optimizing the choice of the cross-linking agent, the monomer/solvent ratio and the sodium salt concentration. The GPE proposed in this work, finally, appears as a compromise between liquid and solid electrolytes, with promising perspectives of application in real system after further optimization.

4. Acknowledgments

Financial support from the French National Research Agency (Project Labex STORE-EX, ANR-10-LABX-76-01) is gratefully acknowledged. We thank Sartomer® for their cross-linking agent and thanks PELLENC ENERGY for supporting this research.

ASSOCIATED CONTENT

The Supporting Information is available free of charge at https://..." More details on experimental and characterizations, some detailed equations, additional FTIR spectra, DSC thermograms, additional complex impedance plots, kinetic monitoring of SEI resistance in OCV.

REFERENCES

(1) Xu, K. Electrolytes and Interphases in Li-Ion Batteries and Beyond. *Chem Rev* **2014**, *114* (23), 11503–11618. https://doi.org/10.1021/cr500003w.

(2) Cohn, A. P.; Muralidharan, N.; Carter, R.; Share, K.; Pint, C. L. Anode-Free Sodium Battery through in Situ Plating of Sodium Metal. *Nano Lett* **2017**, *17* (2), 1296–1301. https://doi.org/10.1021/acs.nanolett.6b05174.

(3) Zhou, W.; Li, Y.; Xin, S.; Goodenough, J. B. Rechargeable Sodium All-Solid-State Battery. *ACS Cent Sci* **2017**, *3* (1), 52–57. https://doi.org/10.1021/acscentsci.6b00321.

(4) Roscher, D.; Kim, Y.; Stepien, D.; Zarrabeitia, M.; Passerini, S. Solvent-Free Ternary Polymer Electrolytes with High Ionic Conductivity for Stable Sodium-Based Batteries at Room Temperature. *Batter Supercaps* **2023**. https://doi.org/10.1002/batt.202300092.

(5) Monroe, C.; Newman, J. The Impact of Elastic Deformation on Deposition Kinetics at Lithium/Polymer Interfaces. *J Electrochem Soc* **2005**, *152* (2), A396. https://doi.org/10.1149/1.1850854.

(6) Lee, B.; Paek, E.; Mitlin, D.; Lee, S. W. Sodium Metal Anodes: Emerging Solutions to Dendrite Growth. *Chem Rev* **2019**. https://doi.org/10.1021/acs.chemrev.8b00642.

(7) Khurana, R.; Schaefer, J. L.; Archer, L. A.; Coates, G. W. Suppression of Lithium Dendrite Growth Using Cross-Linked Polyethylene/Poly(Ethylene Oxide) Electrolytes: A New Approach for Practical Lithium-Metal Polymer Batteries. *J Am Chem Soc* **2014**, *136* (20), 7395–7402. https://doi.org/10.1021/ja502133j.

(8) Zhang, W.; Zhang, J.; Liu, X.; Li, H.; Guo, Y.; Geng, C.; Tao, Y.; Yang, Q. H. In-Situ Polymerized Gel Polymer Electrolytes with High Room-Temperature Ionic Conductivity and Regulated Na+ Solvation Structure for Sodium Metal Batteries. *Adv Funct Mater* **2022**, *32* (25), 1–8. https://doi.org/10.1002/adfm.202201205.

(9) Murugan, S.; Klostermann, S. V.; Schützendübe, P.; Richter, G.; Kästner, J.; Buchmeiser, M. R. Stable Cycling of Room-Temperature Sodium-Sulfur Batteries Based on an In Situ Crosslinked Gel Polymer Electrolyte. *Adv Funct Mater* **2022**, *32* (32). https://doi.org/10.1002/adfm.202201191.

(10) Ha, H. J.; Kil, E. H.; Kwon, Y. H.; Kim, J. Y.; Lee, C. K.; Lee, S. Y. UV-Curable Semi-Interpenetrating Polymer Network-Integrated, Highly Bendable Plastic Crystal Composite Electrolytes for Shape-Conformable All-Solid-State Lithium Ion Batteries. *Energy Environ Sci* **2012**, *5* (4), 6491–6499. https://doi.org/10.1039/c2ee03025j.

(11) Yang, Z.; Peng, H.; Wang, W.; Liu, T. Efficiency of 2,2-Dimethoxy-2-Phenylacetophenone for the Photopolymerization of Methacrylate Monomers in Thick Sections. *J Appl Polym Sci* **2010**, *116* (5), 2658–2667. https://doi.org/10.1002/app.

(12) Hoti, G.; Caldera, F.; Cecone, C.; Pedrazzo, A. R.; Anceschi, A.; Appleton, S. L.; Monfared, Y. K.; Trotta, F. Effect of the Cross-Linking Density on the Swelling and Rheological Behavior of Ester-Bridged β-Cyclodextrin Nanosponges. *Materials* **2021**, *14* (3), 478.

(13) Tchitchekova, D. S.; Monti, D.; Johansson, P.; Bardé, F.; Randon-Vitanova, A.; Palacín, M. R.; Ponrouch, A. On the Reliability of Half-Cell Tests for Monovalent (Li + , Na +) and Divalent (Mg 2+ , Ca 2+) Cation Based Batteries . *J Electrochem Soc* **2017**, *164* (7), A1384–A1392. https://doi.org/10.1149/2.0411707jes.

(14) Studer, K.; Decker, C.; Beck, E.; Schwalm, R. Overcoming Oxygen Inhibition in UV-Curing of Acrylate Coatings by Carbon Dioxide Inerting, Part I. *Prog Org Coat* **2003**, *48* (1), 92–100. https://doi.org/10.1016/S0300-9440(03)00120-6.

(15) DECKER, C. Polymérisation Sous Rayonnement UV. *Technique de l'ingénieur* **2000**. https://doi.org/10.51257/a-v1-am3044.

(16) Patacz, C.; Coqueret, X.; Decker, C. Electron-Beam Initiated Polymerization of Acrylate Compositions 3: Compared Reactivity of Hexanediol and Tripropyleneglycol Diacrylates under UV or EB Initiation. *Radiation Physics and Chemistry* **2001**, *62* (5–6), 403–410. https://doi.org/10.1016/S0969-806X(01)00209-2.

(17) Chuda, K.; Smolinski, W.; Defoort, B.; Rudz, W.; Gawdzik, B.; Rayss, J.; Coqueret, X. Effects of Vitrification on the Isothermal Polymerization of Acrylate Blends under Radiation. *Polimery/Polymers* **2004**, *49* (7–8), 505–513. https://doi.org/10.14314/polimery.2004.505.

(18) Barszczewska-Rybarek, I. M. Quantitative Determination of Degree of Conversion in Photocured Poly(Urethane-Dimethacrylate)s by Fourier Transform Infrared Spectroscopy. *J Appl Polym Sci* **2012**, *123* (3), 1604–1611. https://doi.org/10.1002/app.34553.

(19) choudhury, S.; Saha, T.; Naskar, K.; Stamm, M.; Heinrich, G.; Das, A. A Highly Stretchable Gel-Polymer Electrolyte for Lithium-Sulfur Batteries. *Polymer (Guildf)* **2017**, *112*, 447–456. https://doi.org/10.1016/j.polymer.2017.02.021.

(20) Zhang, L.; Chaloux, B. L.; Saito, T.; Hickner, M. A.; Lutkenhaus, J. L. Ion Conduction in Poly(Ethylene Oxide) Ionically Assembled Complexes. *Macromolecules* **2011**, *44* (24), 9723–9730. https://doi.org/10.1021/ma201715s.

(21) Wong, D. H. C.; Thelen, J. L.; Fu, Y.; Devaux, D.; Pandya, A. A.; Battaglia, V. S.; Balsara, N. P.; DeSimone, J. M. Nonflammable Perfluoropolyether-Based Electrolytes for Lithium Batteries. *Proc Natl Acad Sci U S A* **2014**, *111* (9), 3327–3331. https://doi.org/10.1073/pnas.1314615111.

(22) Cheng, H.; Zhu, J.; Jin, H.; Gao, C.; Liu, H.; Cai, N.; Liu, Y.; Zhang, P.; Wang, M. In Situ Initiator-Free Gelation of Highly Concentrated Lithium Bis(Fluorosulfonyl)Imide-1,3-Dioxolane Solid Polymer Electrolyte for High Performance Lithium-Metal Batteries. *Mater Today Energy* **2021**, *20*, 100623. https://doi.org/10.1016/j.mtener.2020.100623.

(23) Zheng, J.; Dang, H.; Feng, X.; Chien, P. H.; Hu, Y. Y. Li-Ion Transport in a Representative Ceramic-Polymer-Plasticizer Composite Electrolyte: Li7La3Zr2O12-Polyethylene Oxide-Tetraethylene Glycol Dimethyl Ether. *J Mater Chem A Mater* **2017**, *5* (35), 18457–18463. https://doi.org/10.1039/c7ta05832b.

(24) Jae-chang Seol, Ramkumar Balasubramaniam, Vanchiappan Aravindan, Ranjith Thangavel, Y.-S. L. Ameliorating the Electrode/Electrolyte Interface Compatibility in Li-Ion Solid-State Batteries with Plasticizer. *J Alloys Compd* **2022**, *927*. https://doi.org/10.1016/j.jallcom.2005.05.002.

(25) Johansson Patrik; Gejji Shridhar P.; Tegenfeldta JoÈrgen; Lindgrena Jan. The Imide Ion: Potential Energy Surface and Geometries. *Electrochim Acta* **1998**, *43*, 1375–1379.

(26) Moreno, J. S.; Armand, M.; Berman, M. B.; Greenbaum, S. G.; Scrosati, B.; Panero, S. Composite PEOn:NaTFSI Polymer Electrolyte: Preparation, Thermal and Electrochemical Characterization. *J Power Sources* **2014**, *248*, 695–702. https://doi.org/10.1016/j.jpowsour.2013.09.137.

(27) Golitsyn, Y.; Pulst, M.; Samiullah, M. H.; Busse, K.; Kressler, J.; Reichert, D. Crystallization in PEG Networks: The Importance of Network Topology and Chain Tilt in Crystals. *Polymer (Guildf)* **2019**, *165* (28), 72–82. https://doi.org/10.1016/j.polymer.2019.01.018.

(28) Klein, R. J.; Zhang, S.; Dou, S.; Jones, B. H.; Colby, R. H.; Runt, J. Modeling Electrode Polarization in Dielectric Spectroscopy: Ion Mobility and Mobile Ion Concentration of Single-Ion Polymer Electrolytes. *Journal of Chemical Physics* **2006**, *124* (14). https://doi.org/10.1063/1.2186638.

(29) Bocharova, V.; Sokolov, A. P. Perspectives for Polymer Electrolytes: A View from Fundamentals of Ionic Conductivity. *Macromolecules* **2020**, *53* (11), 4141–4157. https://doi.org/10.1021/acs.macromol.9b02742.

(30) Boschin, A.; Johansson, P. Characterization of NaX (X: TFSI, FSI) - PEO Based Solid Polymer Electrolytes for Sodium Batteries. *Electrochim Acta* **2015**, *175*, 124–133. https://doi.org/10.1016/j.electacta.2015.03.228.

(31) Liu, L.; Qi, X.; Yin, S.; Zhang, Q.; Liu, X.; Suo, L.; Li, H.; Chen, L.; Hu, Y. S. In Situ Formation of a Stable Interface in Solid-State Batteries. *ACS Energy Lett* **2019**, *4* (7), 1650–1657. https://doi.org/10.1021/acsenergylett.9b00857.

(32) Evans, J.; Vincent, C. A.; Bruce, P. G. Electrochemical Measurement of Transference Numbers in Polymer Electrolytes. *Polymer (Guildf)* **1987**, *28* (13), 2324–2328. https://doi.org/10.1016/0032-3861(87)90394-6.

(33) Masayoshi WATANABE, Satoshi NAGANO, K. S. and N. O. ESTIMATION OF Li+ TRANSPORT NUMBER IN POLYMER ELECTROLYTES BY THE COMBINATION OF COMPLEX IMPEDANCE AND POTENTIOSTATIC POLARIZATION MEASUREMENTS. *Solid State Ion* **1988**, *28–30* (PART 2), 911–917.

(34) Peled, E.; Golodnitsky, D.; Ardel, G. Advanced Model for Solid Electrolyte Interphase Electrodes in Liquid and Polymer Electrolytes. *J Electrochem Soc* **1997**, *144* (8), L208–L210. https://doi.org/10.1149/1.1837858.

(35) Wang, Q.; Xu, X.; Hong, B.; Bai, M.; Li, J.; Zhang, Z.; Lai, Y. Molecular Engineering of a Gel Polymer Electrolyte via In-Situ Polymerization for High Performance Lithium Metal Batteries. *Chemical Engineering Journal* **2022**, *428*, 131331. https://doi.org/10.1016/j.cej.2021.131331.

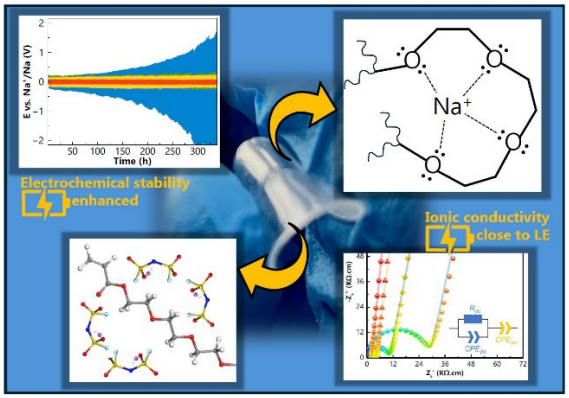
E vs. Na+/Na (V)
Time (h)
Electrochemical stability
enhanced
Na+
Ionic conductivity
close to LE